Journal of Applied Polymer Science

Formation and Structure of Polytetrafluoroethylene Fibrils

Zhang Dong-na, Kou Kai-chang, Zhang Yu, Zhao Qing-xin, Zheng Zhen-chao
Key Laboratory of Macromolecular Science & Technology of Shaanxi Province, Northwestern Polytechnical University, Xi'an 710129, China
Correspondence to: Zhang Dong-na, E - mail: (zhangdongna112@gmail.com)

ABSTRACT: Polytetrafluoroethylene (PTFE) is a semi-crystalline polymer whose fibrils can be easily formed by stretching because of its low tensile activation energy. We prepared two series of PTFE samples with different elongations and degrees of crystallinity, respectively. The morphology analysis of the first series determined that cavities were formed in the PTFE matrix under stretching, and this was a prerequisite for forming fibrils. The barrier between cavities became long and slim under tension, and grew into fibrils finally. It could be found that higher crystallinity is more suitable for forming fibrils. The main part of the fibrils' structure was semi-crystalline, and the degree of crystallinity could grow under stretching. Besides, the thickness of the lamellae decreased, while the crystalline grain refined at the same time. In the measurement of X-ray diffraction, it could be found that the lattice plane (108) was more sensitive to stretching, which could rotate to other positions. © 2013 Wiley Periodicals, Inc. J. Appl. Polym. Sci. 130: 3710–3717, 2013

KEYWORDS: porous materials; crystallization; differential scanning calorimetry

Received 26 April 2013; accepted 7 June 2013; Published online 27 June 2013
DOI: 10.1002/app.39630

INTRODUCTION

Polytetrafluoroethylene (PTFE) is a completely symmetrical, linear polymer. PTFE lamella is formed by folded chain, and owing to the low polarizability of fluorine atom, the intermolecular forces between PTFE chains are fairly weak,[1–3] so the lamella is easy to glide. Besides, tensile activation energy of PTFE is 11.3 kJ/mol,[4] which enables the formation of PTFE fibrils at a low temperature by stretching.[5,6] Expanded PTFE(ePTFE)[7,8] is one of the products prepared by stretching, and it is used in a multitude of clinical and biomedical applications. ePTFE is remarkably flexible and its mechanical properties depend on the microstructure of the expanded polymer foam,[9] which is made of fibrils and node.[10]

Investigation of morphological structures and deformation in drawn PTFE has been carried out by many researchers, and there has been comment on the presence of fibrils, which play an important role in the performance of drawn PTFE. Okuyama[11] used wide angle X-ray line broadening to measure individual fibril, which showed that the diameter of fibril was corresponding to the crystalline domain size along the chain axis. Brown[12] suggested that the stability of drawing fibrils was primarily determined by temperature and the crystalline phase with additional dependence on loading rate and microstructure anisotropy. Other semi-crystalline polymers, such as polyethylene,[13] polypropylene,[14,15] and nylon,[16] also exhibit the process of forming fibril during tension, but researchers paid more attention on the transformation of crystal.

Fibril nucleate from the point of stress concentration, and can dissipate energy and stabilize a crack tip by bridging,[17,18] therefore, there is a considerable interest in the structure of fibrils. O'Leary[19] measured the structure of fibril by electron diffraction, and believed that it was a large perfect, low molecular weight crystal. Then Kitamura[6] suggested that fibril formation was a process of unraveling of the crystalline domains, and still was a crystalline structure in the direction of loading. But Ariawan[20] believed that fibrils were oriented amorphous PTFE formed by unwinding of the crystalline domains.

It can be detected that the microstructure of PTFE fibrils requires further investigation. One of the discussions is whether the fibril was crystalline or noncrystalline. Based on that, drawn PTFE in different tensile ratios were prepared at room temperature, and through this series of samples, the growing process of PTFE fibrils could be detected. Besides, drawn samples in different crystallinity were also measured to demonstrate the structure of fibrils.

EXPERIMENTAL

Sample Preparation

PTFE powder used in this study was from 3F Floro-Chemical, Shandong, China. It was molded into specimens bar at 50 MPa for 10 min at room temperature. The molded samples were

Table I. Lengths of the Marked Part Before Unloading and After Placed for 48 h

Sample	FD-0	FD-1	FD-2	FD-3	FD-4	FD-5
Length of marked part before unloading (mm)	10.0	12.0	15.0	18.0	21.0	24.0
Length of marked part placed for 48 h (mm)	10.0	10.8	11.5	12.8	14.3	15.9

heated to 375°C at 10°C/min, maintained for 2 h to allow the particles coalesced completely, and then cooled to room temperature. Samples in different degrees of crystallinity were prepared through different annealing processes. There were four kinds of anneal, and they were cooled in the mixture of water and ice, cooled in air at 20°C, natural cooled in the furnace and cooled at the speed of 10°C/min separately. The four annealing processes were marked as A, B, C, and D.

Specimen D was stretched unaxially in different strain ratios at the speed of 10 mm/min at 25°C. Necking phenomenon was not happened during this process, so the middle area of the specimen could be regarded as uniform elongation.[21] We marked out the middle part of 10 mm, which were tested before unloaded the tension, and it was also measured after placed for 48 h at room temperature. Both of the lengths were listed in Table I. Specimens D with different elongations were denoted as FD-0, FD-1, FD-2, FD-3, FD-4, and FD-5. The tensile ratio of samples in different degrees of crystallinity was the same as FD-4's, and they were marked as FA-4, FB-4, and FC-4.

Scanning Electron Microscopy

Morphology of specimens in different tensile ratios were examined by VEGA3 LMH scanning electron microscopy (SEM), operated in vacuum mode. Samples were cooled in liquid nitrogen before rupture, and the surface was given a coating of gold about 5-nm thick. Surfaces to be observed were parallel and perpendicular to the tension direction.

Crystallization Behavior Measurements

Different scanning calorimetry (DSC) was performed with a TA Instruments Q1000 system at a heating/cooling rate of 10°C/min under a nitrogen atmosphere. Sample of 10 mg was taken from the marked area, and heated from room temperature to 380°C. X-ray diffraction (XRD) tested on X'Pert PRO MPD Diffractometer (Cu Kα radiation with $\lambda = 0.15406$ nm operated at 40 kV and 35 mA). The range of 2θ was from 10° to 50° at a rate of 5°/min. XRD was used to study the structural parameters of the matrix with different crystallinity and tension ratios.

RESULTS AND DISCUSSION

The Formation of Fibrils

The process of fibrils' formation has received great interest in the literature. Although the precise structure of fibrils was still unclear, estimates of the mechanical strength and stiffness of individual fibrils are consistently greater than the bulk.[11,12] Figure 1(a) is the SEM images of FD-5 perpendicular to tension direction, whereas Figure 1(b) is parallel to the stretching direction. The orientated beam can be detected in Figure 1(b), and the plane of Figure 1(a) is flat. Orientation brought a remarkable difference to the material, and fibrosis structure could be found in the orientated beam, which was shown in Figure 2.

Figure 2 is the SEM images of FD-0, FD-2, FD-4, and FD-5, whose fracture plane was parallel to the tension direction, and Figure 2(a) is that of FD-0, it was compact and uniform. When the drawn ratio increased, voids began to nucleate. When Figure 2(b,c,d) is compared, there is less void in Figure 2(b), besides, fibrils can be found in the last two images. In Figure 2(d), a great deal of void and fibrils were formed not only in the surface, but also in the matrix. It was believed that the formation of voids and fibrils was associated, and fibrils could form when the quantity and size of the voids were large enough.

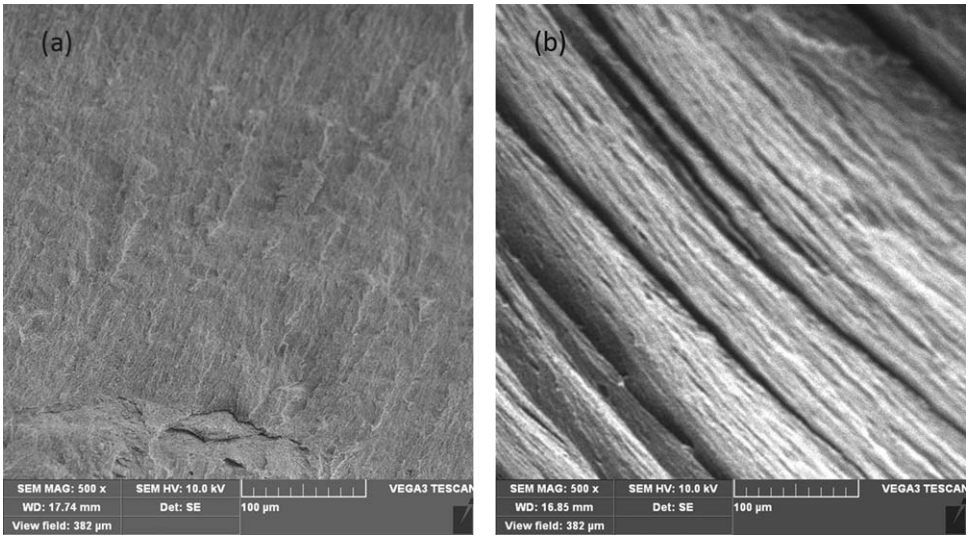

Figure 1. SEM images of fracture plane morphology for FD-5 perpendicular and parallel to stretching direction.

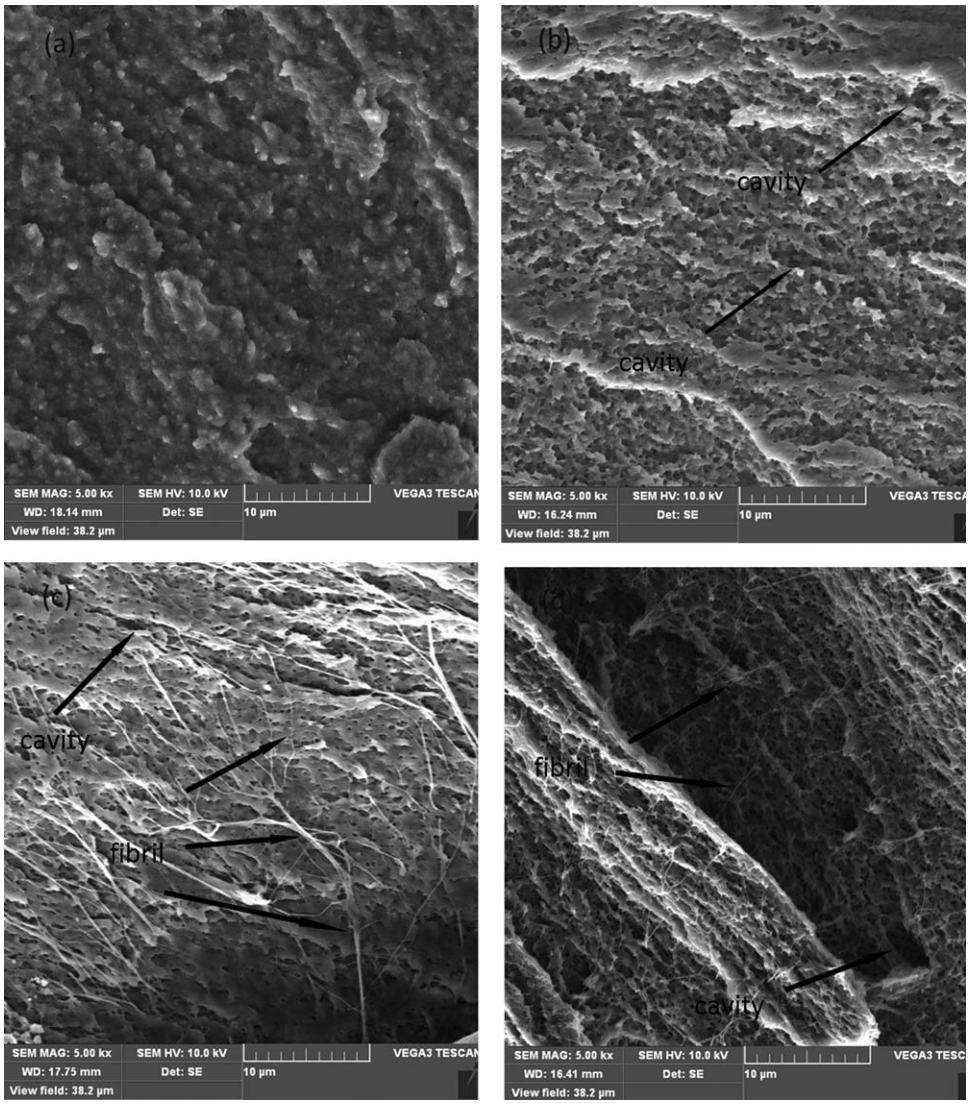

Figure 2. SEM images of fracture plane morphology for FD-0, FD-2, FD-4, and FD-5 parallel to tension direction.

Two images in Figure 3 were both for FD-5 with the same magnification, but morphology of the two differed widely. Figure 3(a) is the image paralleled to the tension direction, and voids and fibril can be found because of the orientation. Voids might nucleate from the points of stress concentration, and with further elongation, voids became longer along the stress direction. The barrier between the holes stretched, became slender, and grew into fibrils finally. In Figure 3(b), the surface of resin looks like hills with cavities in. Three-dimensional reticular structure was built by tension, whose bone was PTFE fibrils or ligaments.

It can be found from the SEM images that, the growing process of fibril is started by the forming of voids and intensified by orientation. The barrier between the voids becomes longer with stretching, besides, the strength of PTFE is high, and it cannot break until a certain degree. The drawn sample was much looser than the native one, and density of the specimens was measured according to ASTM792–2000, which shown in Table II. From the results of density, porosity (P) of each sample could be calculated by eq. (1). In this formula, ρ is the density of the drawn sample, and ρ_0 is the density of FD-0, which is considered being absolutely dense. The increasing porosity reveals the growing of void and fibrils in PTFE. Generally speaking, higher degree of crystallinity brings the material higher density, and in this discussion, ρ_0 was all taken as 2.172 from FD-1 to FD-5. As a result of the neglect of change in density, porosities calculated through eq. (1) was less than the actual value, but the increasing trend was unalterable. As we know, PTFE is widely used in sealing, and high porosity might improve the compressibility, which could ensure initial sealing under pre-tightening force.

$$P=\left(1-\frac{\rho}{\rho_0}\right)\times 100\% \quad (1)$$

The Structure of Fibrils

As we discussed above, the structure of fibrils was still unclear, and one discussion is whether it was crystalline or

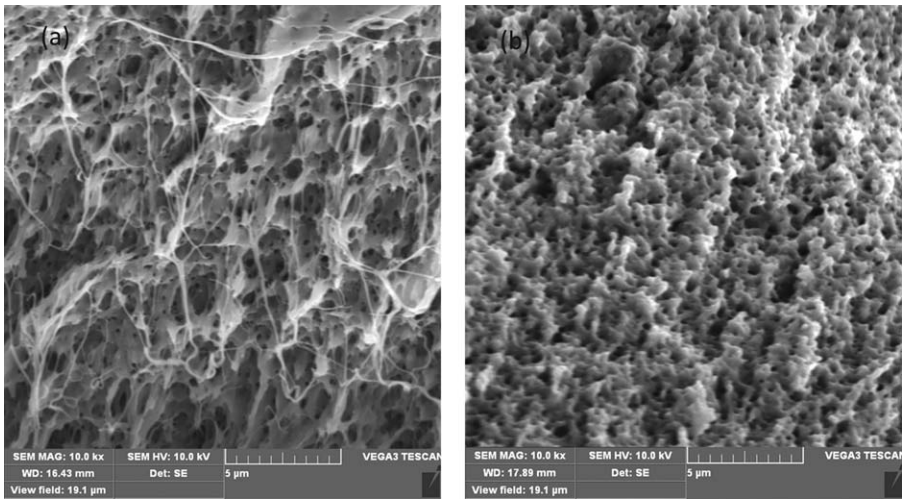

Figure 3. SEM images of fracture plane morphology for FD-4 parallel and perpendicular to tension direction.

noncrystalline. In this section, DSC and XRD were employed to study the structure of fibrils. In order to determine the degree of crystallinity from DSC measurements, melting enthalpy(ΔH_m^0) for 100% crystalline material was taken as 69 J/g[22] and the following equation was used:

$$X_c = \frac{\Delta H_m(\text{sample})}{\Delta H_m^0} \quad (2)$$

Besides, the change of crystal structure and growth process of fibril was investigated. PTFE in different degrees of crystallinity were observed. Four kinds of samples were prepared through different annealing processes, which were cooled in mixture of water and ice (A), cooled in air at 20°C (B), natural cooled in furnace (C), and cooled with the speed of 10°C/min (D) separately. The DSC curves of samples before and after stretching were shown in Figure 4, and the result was shown in Table III.

Through Table III, it can be found that the degree of crystallinity calculated by two methods show the same trend. The effect of anneal was remarkable, and crystallinity degree of PTFE after stretching were all improved. Orientation was benefit for crystallizing, although the tensile temperature was below the glass transition temperature, the role of stress-induced could not be ignored. Peak temperature (T_p), fusion onset, and end temperature of this series of sample were shown in Figures 5 and 6.

T_p was determined to be fusion temperature (T_m), and the value between onset temperature and end temperature was marked as $T_{(\text{endset-onset})}$. It can be found from Figures 4–6 that, with the cooling degree retarded, T_m increased and $T_{(\text{endset-onset})}$ decreased. Mild cooling process was benefit for the growth of lamella thickness and the improving of crystal perfection.

Table II. Density and Porosity of PTFE Samples in Different Draw Ratios

Sample	FD-0	FD-1	FD-2	FD-3	FD-4	FD-5
Density (g/cm^3)	2.172	2.164	2.134	2.065	2.011	1.908
Porosity (%)	0	0.37	1.75	4.93	7.41	12.15

It could be detected that the perfection degree of crystal improved under tension, and all of the T_m were decreased after stretching, which showed that the lamellae thickness was

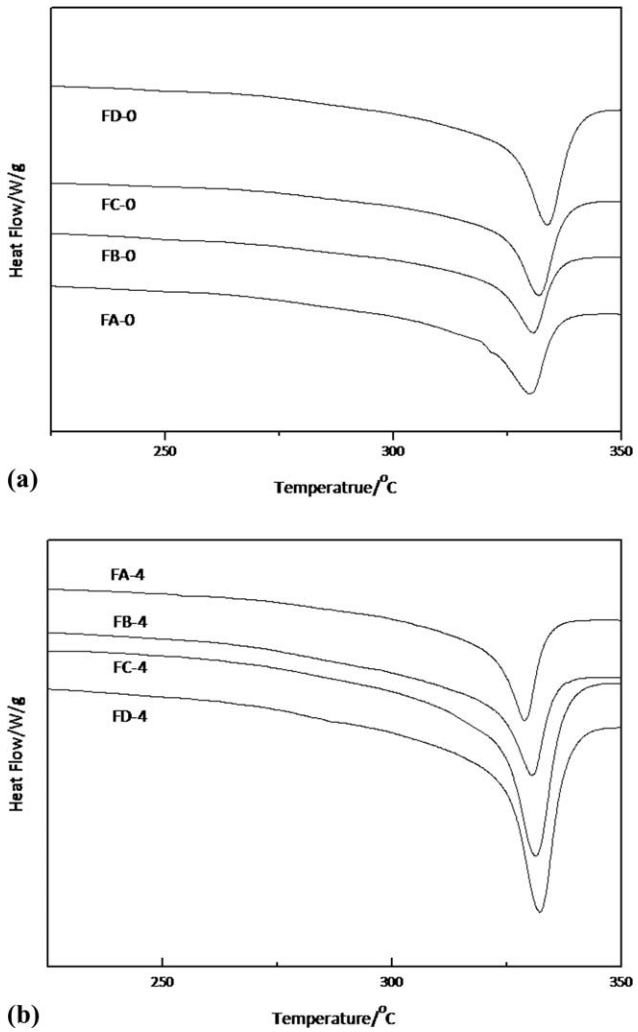

Figure 4. DSC curve of PTFE samples in different cooling processes.

Table III. Degree of Crystallinity of PTFE in Different Cooling Processes Before and After Stretching

	FA		FB		FC		FD	
Sample	FA-0	FA-4	FB-0	FB-4	FC-0	FC-4	FD-0	FD-4
Degree of crystallinity(%)/XRD	22.01	24.26	27.88	31.41	31.85	35.23	36.94	41.88
Degree of crystallinity(%)/DSC	30.24	32.14	34.52	37.78	40.48	48.06	45.23	56.84

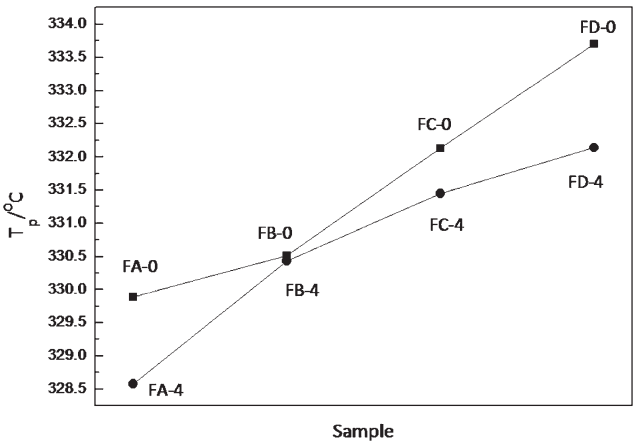

Figure 5. T_p of PTFE in different cooling processes before and after stretching.

refined.[24] Degree of crystallinity was easier to be enhanced under stretching when it was higher in the nonstretched one. From the SEM images of drawn PTFE, it can be found that lots of fibrils were formed. PTFE sample was semi-crystalline, and the growing of crystallinity degree was accompanied with the formation of fibrils. Density of each sample was shown in Table IV, and the porosity was shown in Figure 7. Density of samples before stretching in different cooling processes was increased, and densities after stretching were almost the same. Because the increasing porosity made density decreased, whereas higher degree of crystallinity made it increased. Porosity was calculated by eq. (1), and it was improved from sample FA-4 to FD-4. The SEM images of FA-4 and FC-4 are shown in Figure 8. More cavities could be found in Figure 8(b). It can be observed that higher degree of crystallinity is beneficial to form cavities. As discussed above, cavity was the precondition of the formation fibrils, so it could infer that higher degree of crystallinity was benefit for forming fibrils and the main component of fibrils was crystalline. Brown[25] compared the efficiency in fibril formation between 53% and 62% crystalline PTFE, and suggested that the formation process was restricted by the increase in crystallinity. This conclusion was in contradiction with ours, but crystallinity of samples in our discussion was lower, and the discussion range of crystallinity was different.

Figure 9 is the XRD patterns of samples with different degree of crystallinity before and after stretching. In Figure 9(a), differences between the four patterns were the diffraction peaks intensity around 37° and 41°. The increasing peak intensity showed the improvement of crystallinity degree, and the result was

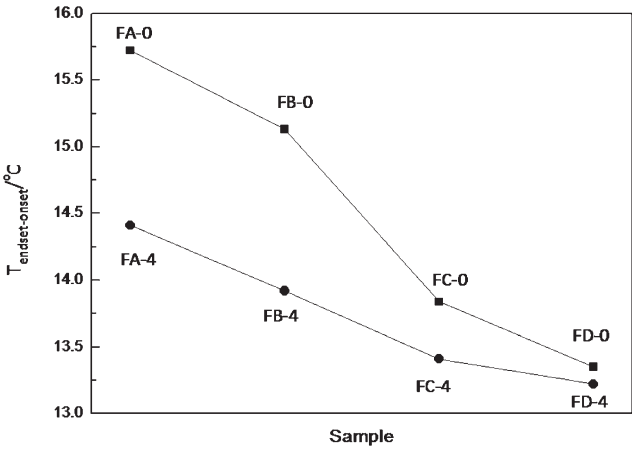

Figure 6. $T_{endset-onset}$ of PTFE in different cooling processes before and after stretching.

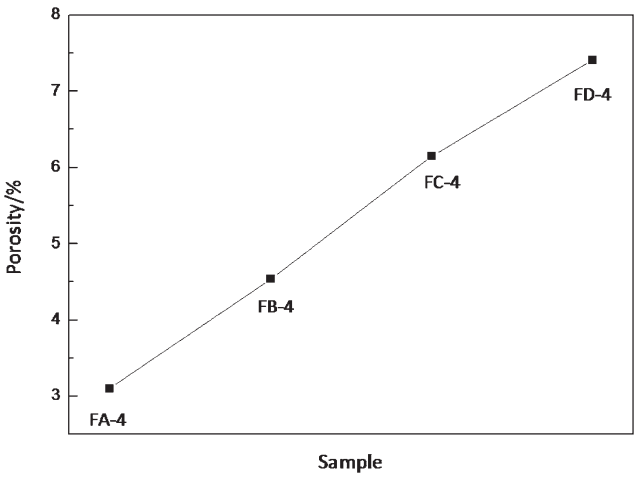

Figure 7. Porosity of PTFE samples in different cooling processes.

Table IV. Density of PTFE Samples in Different Cooling Processes Before and After Stretching

Sample	FA-0	FA-4	FB-0	FB-4	FC-0	FC-4	FD-0	FD-4
Density	2.062	1.998	2.097	2.002	2.121	1.991	2.172	2.011

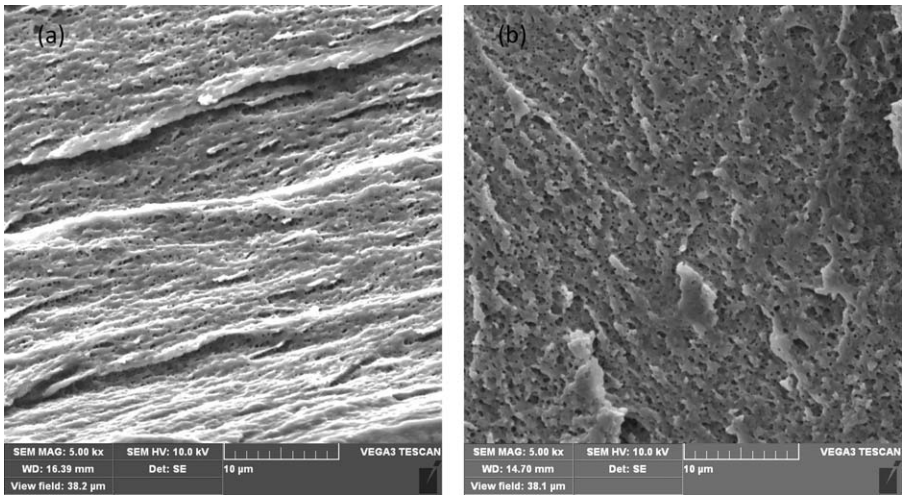

Figure 8. SEM images of fracture plane morphology for FA-4 and FC-4 parallel to tension direction.

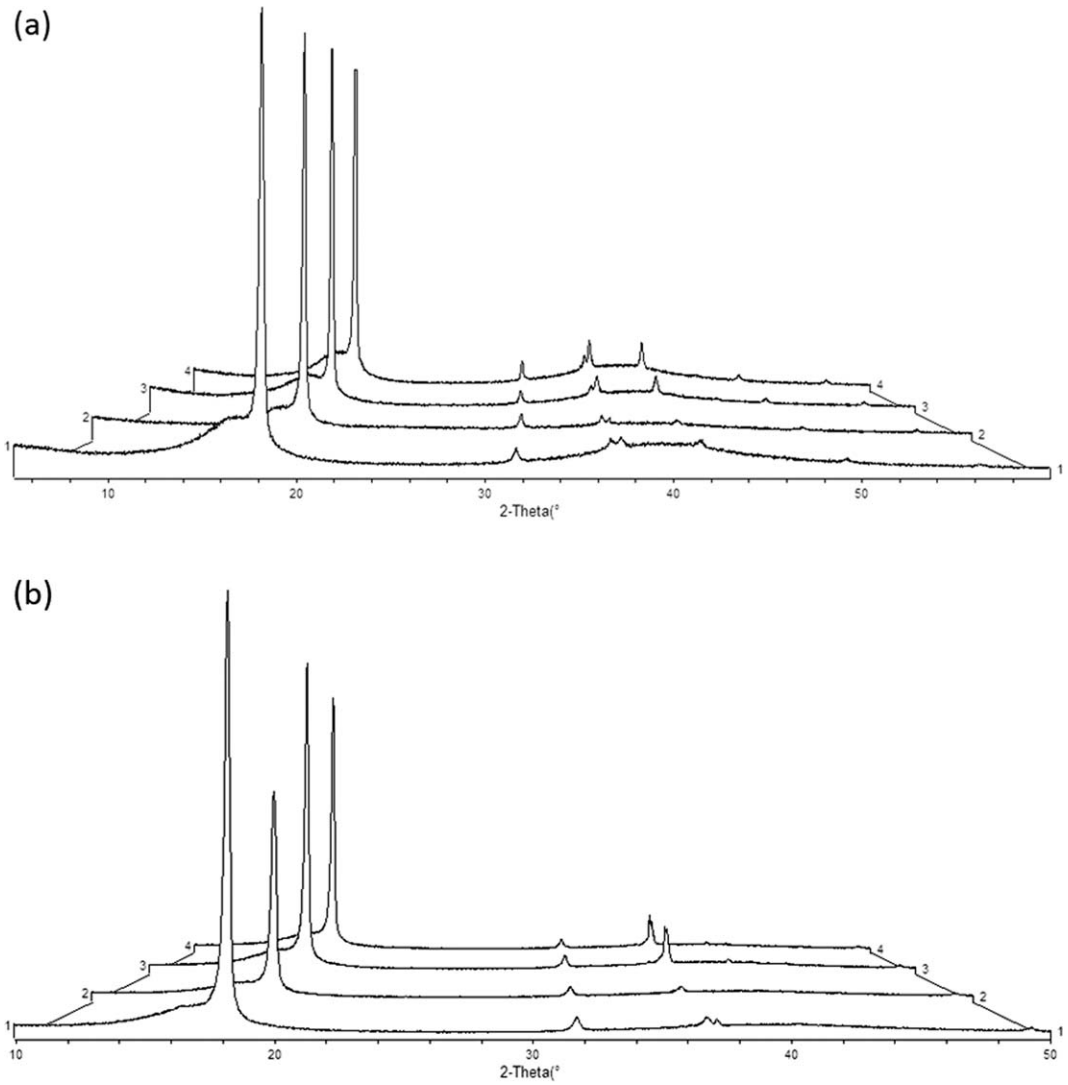

Figure 9. XRD patterns of PTFE sample in different cooling processes: (a) before stretching; and (b) after stretching; (1. FA, 2. FB, 3. FC, 4. FD).

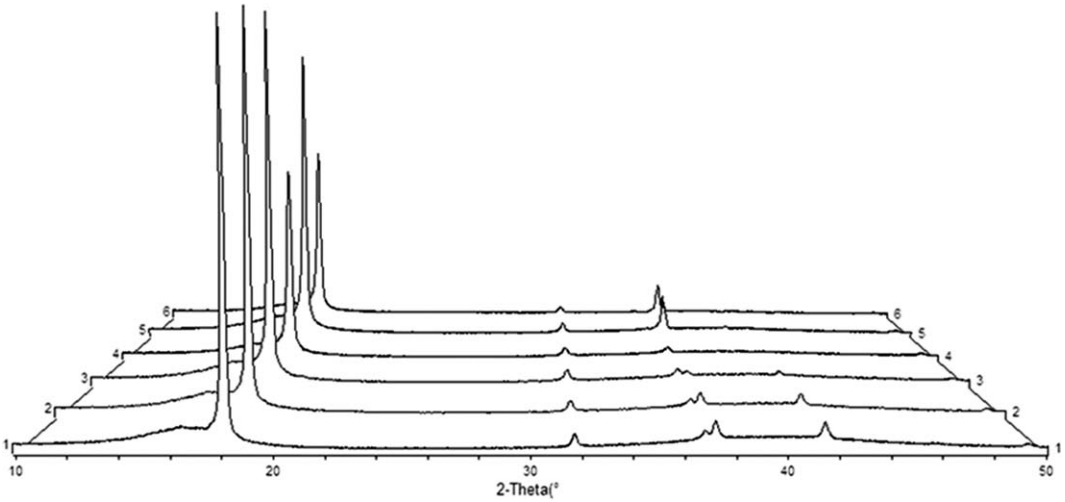

Figure 10. XRD patterns of PTFE sample in different stretching elongations (1. FD-0, 2. FD-1, 3. FD-2, 4. FD-3, 5. FD-4, 6. FD-5).

shown in Table III. After stretching, the two peaks around 37° merged into one peak, which could be found in samples FB-4, FC-4, and FD-4, and diffraction peak at 41° disappeared. The miller index of peak at 41° is (108), and this crystal structure was easy to be destroyed. Peak intensity around 37° (107) improved a lot because of the orientation. It could be obtained that the lattice plane (108) was more sensitive to stretching, and it was rotated to other positions. The lattice plane (107) was strengthened. Besides, higher degree of crystallinity was a benefit for the crystal transition during the process of stretching. Peak intensity of FC-4 and FD-4 around 37° increased obviously compared with the other two samples.

In this discussion, it could be found that PTFE fibrils were imperfect crystal. The change of peak intensities showed stretching brought a remarkable effect to the crystal structure of PTFE. Higher degree of crystallinity was more sensitive to the crystal transition, and combined with the SEM images, it could be suggested that, higher degree of crystallinity is more suitable to form fibrils, which agrees with the analysis of DSC.

Sample FD-0 with different elongations was marked as FD-1, FD-2, FD-3, FD-4, and FD-5, and the XRD patterns were shown in Figure 10. The mill index of peaks, around 36° and 37°, are (107) and (200), respectively. From FD-0 to FD-5, the two peaks broaden gradually and superposed to be one peak, whose peak intensity grew gradually. The relative intensity of diffraction peak around 41° is weak, but it can be found in patterns 1–3 easily, which is corresponding to the samples FD-0–FD-2. Increasing the tension ratio, this peak becomes weaker and finally disappeared. Those two changes pointed out a same phenomenon, which was grain refinement. Lemine[26] believed that peak broadening could be caused by a reduction in crystallite size. In the analysis of DSC, T_m deceased after tension. The grain in PTFE or PTFE fibril or even in both became smaller with stretching. But this process should not be endless because further tension may destruct the fibril and the composite.

As discussed in this paper, the structure of fibrils was imperfect semi-crystalline. Higher crystallinity degree was beneficial to form fibrils, and crystallinity of fibrils and matrix improved under stretching. Crystals of fibrils were more homogenous than the bulk. Lamellae thickness and grain size were decreased in fibril under tension.

CONCLUSIONS

In this article, we investigated the formation and structure of PTFE fibrils that formed under stretching at room temperature. Samples with different elongations were used to study the formation process of fibrils. It could be found that cavities or voids were formed in the resin matrix first. And then, with the increase of elongation, the length of the barrier between voids grew along the orientation of the extension and, eventually, PTFE fibrils were formed. The thickness of lamellae became thinner and the perfection degree of crystal improved after stretching. From the test of crystalline, we detected that higher degree of crystallinity facilitates the formation of fibrils. Fibrils were semi-crystal, and the degree of crystallinity of fibrils could be improved by further stretching. In addition, the grain of crystalline could be refined simultaneously.

REFERENCES

1. Brown, E. N.; Rae, P.; Dattelbaum, D.; Clausen, B.; Brown, D. *Exp. Mech.* **2008**, *48*, 119.
2. Brown, E. N.; Dattelbaum, D.; Brown, D.; Rae, P.; Clausen, B. *Polymer* **2007**, *48*, 2531.
3. Brown, E. N.; Clausen, B.; Brown, D.; *J. Neu. Res.* **2007**, *15*, 139.
4. Kitamura, T.; Kurumada, K. I.; Tanigaki, M.; Ohshima, M.; Kanazawa, S. I. *Polym. Eng. Sci.* **2004**, *39*, 2256.
5. Aderikha, V.; Shapovalov, V. *Wear* **2010**, *268*, 1455.
6. Kitamura, T.; Okabe, S.; Tanigaki, M.; Kurumada, K. I.; Ohshima, M.; Kanazawa, S. I. *Polym. Eng. Sci.* **2004**, *40*, 809.
7. Caddock, B.; Evans, K. *Biomaterials* **1995**, *16*, 1109.

8. Yamada, K.; Ebihara, T.; Gondo, T.; Sakasegawa, K.; Hirata, M. *J. Appl. Polym. Sci.* **1998**, *61*, 1899.
9. Catanese, J.; Cooke, D.; Maas, C.; Pruitt, L. *J. Biomed. Mater. Res.* **1999**, *48*, 187.
10. Gore, R. W. 1976 U.S. *Patent*, 3953566.
11. Okuyama, H.; Kanamoto, T.; Porter, R. *J. Mater. Sci.* **1994**, *29*, 6485.
12. Brown, E. N.; Dattelbaum, D. M. *Polymer* **2005**, *46*, 3056.
13. Godshall, D.; Wilkes, G.; Krishnaswamy, R. K.; Sukhadia, A. M. *Polymer* **2003**, *44*, 5397.
14. Li, X.; Wu, H.; Wang, Y.; Bai, H.; Liu, L.; Huang, T. *Mater. Sci. Eng. A Struct.* **2010**, *527*, 531.
15. Thio, Y.; Argon, A.; Cohen, R.; Weinberg, M. *Polymer* **2002**, *43*, 3661.
16. Wilbrink, M.; Argon, A.; Cohen, R.; Weinberg, M. *Polymer* **2001**, *42*, 10155.
17. Sun, B.; Hsiao, C. *J. Appl. Phys.* **1985**, *57*, 170.
18. Marissen, R. *Polymer* **2000**, *41*, 1119.
19. O'Leary, K.; Geil, P. *J. Appl. Phys.* **1967**, *38*, 4169.
20. Ariawan, A. B.; Ebnesajjad, S.; Hatzikiriakos, S. G. *Polym. Eng. Sci.* **2002**, *42*, 1247.
21. Gan, Y.; Chu, F.; Aglan, H.; Faughnan, P.; Bryan, C. *J. Mater. Sci. Lett.* **2001**, *20*, 581.
22. Wang, Z. C.; Kou, K. C.; Chao, M.; Bi, H.; Yan, L. K. *J. Appl. Polym. Sci.* **2010**, *117*, 1218.
23. Jordan, J. L.; Siviour, C. R.; Foley, J. R.; Brown, E. N. *Polymer.* **2007**, *48*, 4184.
24. Weeks, J. J. *J. Res. Natl Bur. Stand. A* **1963**, *67*, 441.
25. Brown, E. N.; Rae, P. J.; Bruce, O. E.; Gray G. T.; Dattelbaum D. M. *Mater. Sci. Eng.: C* **2006**, *26*, 1338.
26. Lemine, O. *Superlattice. Microst.* **2009**, *45*, 576.